A SHIFT-INVARIANT MULTISCALE MULTIDIRECTION IMAGE DECOMPOSITION

Truong T. Nguyen and Soontorn Oraintara

Dept. of Electrical Engineering, University of Texas at Arlington, 416 Yates St., Arlington, TX, 76019
Email:nttruong@msp.uta.edu, oraintar@uta.edu

ABSTRACT

This paper presents a shift-invariant complex directional pyramid transform constructed by a dual-tree pyramidal directional filter banks (DFB). The double filter bank framework consists of a shift-invariant Laplacian pyramid and a dual-tree DFB. The two binary tree structure for the (primal and dual) DFBs employed in the structure are identical except for the filter bank employed at the second level of the dual DFB, where special conditions on the phase of the filters are required. It is proven analytically and experimentally that each pair of corresponding directional filters produced by the primal and dual filter banks are symmetric and anti-symmetric, which can be interpreted as the real and imaginary parts of a complex filter. Therefore, the two subband coefficients can be viewed as the real and imaginary parts of a complex-valued subband image. It is proven that there is no aliasing in the decimated complex-valued signal, which implies that the system is shift-invariant in the energy sense. In addition, the proposed shift-invariant, multiscale, multidirectional image decomposition has two unique characteristics that other shift-invariant decompositions do not possess. First, the directional resolution of the image transform can be arbitrarily high. Secondly, the two-dimensional filter bank is implemented in a separable fashion, which makes the entire structure very computational efficient.

1. INTRODUCTION

Wavelet and filter bank (FB) have been a major research topic in signal processing for the last two decades [1]. The discrete wavelet transform (DWT) has been shown to be an optimal representation of one-dimensional (1-D) piece-wise smooth signals and found widespread use in many signal and image processing applications. However, there are limitations of the separable DWT, namely translation variance and lack of directionality. The shift-variant property of the DWT means that the representation of signal by wavelet coefficients is dependent on the position of the signal. Since the subsampling operators are linear but shift-variant, translation invariance of the transform can not be obtained. However, a reduced form of translation invariance exists, namely energy shift-invariance or 'shiftability'. This will happen if aliasing in the decimated signal is negligible. This condition implies that the frequency spectrum of the signal before being decimated is strictly bandlimited inside a region of less than the Nyquist frequency associated with the downsampling ratio. In [2], the authors stated and proven that energy shift-invariance is equivalent to the possibility of interpolating the original signals from the decimated signals.

Another problems of the DWT is that it has limited angular resolution. For a two-channel FB such as that used in the DWT, the 2-D FB produces four sub-images, which are usually referred to as LL, LH, HL and HH images. The LH and HL images contain features along the horizontal and vertical directions, but the HH image contains diagonal components of both directions. If the directional selectivity of a FB is defined as the ability to extract orientational features into separate images, then the two-channel separable FB has very poor directional selectivity.

This work was supported in part by NSF Grant ECS-0528964.

Notation. Uppercase bold face letters and lowercase bold face letters represent 2×2 square matrices and 2×1 column vectors, respectively. For example, $h(\mathbf{n})$ is a function defined on the 2-D integer lattice $(n_1, n_2)^T$, and $\boldsymbol{\pi}$ is $(\pi, \pi)^T$. The superscripts ^{T} and $^{-T}$ denote the transpose, transpose of the inverse operators, respectively.

$\mathcal{N}(\mathbf{M})$ is defined as the set of integer vectors of the form $\mathbf{Mx}$ where $\mathbf{x} \in [0, 1)^2$. $|\mathbf{M}|$ represents the determinant of the matrix $\mathbf{M}$. The notation $\boldsymbol{\omega}^{\mathbf{M}}$ is defined as

$$\boldsymbol{\omega}^{\mathbf{M}} \triangleq \begin{bmatrix} m_{11}\omega_1 + m_{21}\omega_2 \\ m_{12}\omega_1 + m_{22}\omega_2 \end{bmatrix}, \boldsymbol{M} = \begin{bmatrix} m_{11} & m_{12} \\ m_{21} & m_{22} \end{bmatrix}. \quad (1)$$

This notation is equivalent to $\boldsymbol{M}^T\boldsymbol{\omega}$. For fundamental operations in multidimensional multirate systems, we refer to [3].

The followings are some special matrices that are used to decimate subband images in the paper:

$$\mathbf{Q} = \begin{bmatrix} 1 & 1 \\ 1 & -1 \end{bmatrix}, \mathbf{D}_2 = \begin{bmatrix} 2 & 0 \\ 0 & 2 \end{bmatrix}.$$

2. THE TWO-LEVEL DUAL-TREE FAN FB

In [4], Kingsbury proposed a dual-tree FB structure to implement a dyadic complex DWT. The dual-tree structure consists of two dyadic trees to implement two multiresolution decompositions of the same signal. The filters employed in the two trees are designed in such a way that the aliasing in one branch in the first tree will be approximately cancelled by the corresponding branch in the second tree. If only two scaling (or wavelet) coefficients at the same level in the primal and dual FBs are retained in the synthesis FBs, the whole multirate system is approximately linear time-invariant. The condition on the wavelet filters of the two trees to obtain shift-invariant property is that they are a Hilbert transform pair. The key to this relation is the half-sample phase delay condition between the two lowpass filters employed in the tree [4].

The conventional DFB [5] is created by cascading two-channel FBs in a binary tree. This section discusses how to construct a dual-tree DFB, whose directional filters have similar relations like the Hilbert transform relation in the dual-tree DWT. As an initial step, a dual-tree of two-level fan FB is constructed . A four-band directional FB is created when one cascades two levels of the same prototype of fan FB. Let $H_0(\boldsymbol{z})$ and $H_1(\boldsymbol{z})$ be the two fan filters of the prototype fan FB. The fan filters in the primal DFB in Fig. 1 are given:

$$H_{0a}(\boldsymbol{\omega}) = H_{00a}(\boldsymbol{\omega}) = H_{10a}(\boldsymbol{\omega}) = H_0(\boldsymbol{\omega}), \quad (2)$$

$$H_{1a}(\boldsymbol{\omega}) = H_{01a}(\boldsymbol{\omega}) = H_{11a}(\boldsymbol{\omega}) = H_1(\boldsymbol{\omega}). \quad (3)$$

1-4244-0469-X/06/$20.00 ©2006 IEEE

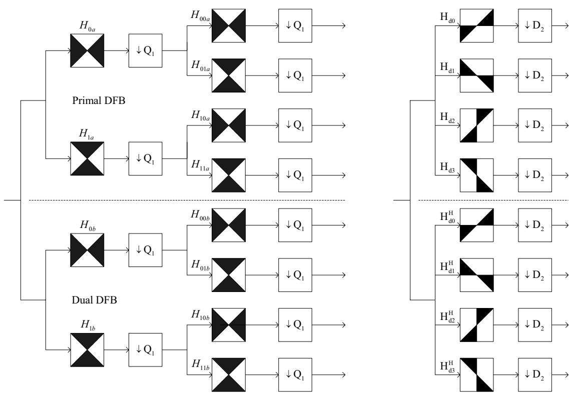

(a) (b)

Fig. 1. The two-level dual-tree fan FB in: (a) the two-level binary tree structure, and (b) the equivalent filter support of the dual-tree of four-channel DFBs.

In Fig. 1(b), the four directional filters $H_{dk}(\boldsymbol{\omega}), k = 0, 1, 2, 3$ are employed in the primal DFB with overall decimation matrix $\boldsymbol{D_2}$. These filters can be related to prototype filters $H_0(\boldsymbol{\omega})$ and $H_1(\boldsymbol{\omega})$ through the tree structure as

$$\begin{aligned} H_{d0}(\boldsymbol{\omega}) &= H_0(\boldsymbol{\omega})H_0(\boldsymbol{\omega}^{\boldsymbol{Q}}), H_{d1}(\boldsymbol{\omega}) = H_0(\boldsymbol{\omega})H_1(\boldsymbol{\omega}^{\boldsymbol{Q}}), \\ H_{d2}(\boldsymbol{\omega}) &= H_1(\boldsymbol{\omega})H_0(\boldsymbol{\omega}^{\boldsymbol{Q}}), H_{d3}(\boldsymbol{\omega}) = H_1(\boldsymbol{\omega})H_1(\boldsymbol{\omega}^{\boldsymbol{Q}}). \end{aligned}$$

The filters on the dual tree are chosen as follow

$$H_{0b}(\boldsymbol{\omega}) = e^{-j\omega_1}H_0(\boldsymbol{\omega}), H_{1b}(\boldsymbol{\omega}) = e^{-j\omega_2}H_1(\boldsymbol{\omega}), \tag{4}$$

$$H_{00b}(\boldsymbol{\omega}) = e^{-j\phi_A(\boldsymbol{\omega})}H_0(\boldsymbol{\omega}), H_{01b}(\boldsymbol{\omega}) = e^{-j\phi_A(\boldsymbol{\omega})}H_1(\boldsymbol{\omega}), \tag{5}$$

$$H_{10b}(\boldsymbol{\omega}) = e^{-j\phi_B(\boldsymbol{\omega})}H_0(\boldsymbol{\omega}), H_{11b}(\boldsymbol{\omega}) = e^{-j\phi_B(\boldsymbol{\omega})}H_1(\boldsymbol{\omega}), \tag{6}$$

where $\phi_A(\boldsymbol{\omega})$ and $\phi_B(\boldsymbol{\omega})$ are phase functions, which will be defined later.

Theorem 1 *Let $A_i(\boldsymbol{z})$ and $B_i(\boldsymbol{z})$ be the analysis and the synthesis filters of channel $i, (i = 0, 1)$ of a quincunx PR FB with a decimation matrix $\boldsymbol{Q}$. If $\phi(\boldsymbol{\omega})$ is a $2\boldsymbol{\pi}$-periodic function satisfying $\phi(\boldsymbol{\omega}) = \phi(\boldsymbol{\omega} + \boldsymbol{\pi})$, then the four filters having frequency responses $e^{-j\phi(\boldsymbol{\omega})}A_0(\boldsymbol{\omega})$, $e^{-j\phi(\boldsymbol{\omega})}A_1(\boldsymbol{\omega})$, $e^{j\phi(\boldsymbol{\omega})}B_0(\boldsymbol{\omega})$ and $e^{j\phi(\boldsymbol{\omega})}B_1(\boldsymbol{\omega})$ render another two-channel PR FB.*

Proof: see [6].

A direct implication of Theorem 1 is that the filters defined in (5)-(6) can be the analysis filters of two fan FBs which are PR as long as $\phi_m(\boldsymbol{\omega}) = \phi_m(\boldsymbol{\omega}+\boldsymbol{\pi}), m \in \{A, B\}$. In this case, the corresponding synthesis filters are modulated by $e^{j\phi_m(\boldsymbol{\omega})}$. Using (4)-(6), the four equivalent filters in the dual tree become:

$$H^H_{d0}(\boldsymbol{\omega}) = e^{-j(\omega_1+\phi_A(\boldsymbol{\omega}^{\boldsymbol{Q}}))}H_{d0}(\boldsymbol{\omega}), \tag{7}$$

$$H^H_{d1}(\boldsymbol{\omega}) = e^{-j(\omega_1+\phi_A(\boldsymbol{\omega}^{\boldsymbol{Q}}))}H_{d1}(\boldsymbol{\omega}), \tag{8}$$

$$H^H_{d2}(\boldsymbol{\omega}) = e^{-j(\omega_2+\phi_B(\boldsymbol{\omega}^{\boldsymbol{Q}}))}H_{d2}(\boldsymbol{\omega}), \tag{9}$$

$$H^H_{d3}(\boldsymbol{\omega}) = e^{-j(\omega_2+\phi_B(\boldsymbol{\omega}^{\boldsymbol{Q}}))}H_{d3}(\boldsymbol{\omega}). \tag{10}$$

The key idea for the construction of the dual-tree of four-channel DFBs is to choose $\phi_A(\boldsymbol{\omega})$ and $\phi_B(\boldsymbol{\omega})$ so that the equivalent directional filters of the dual DFB are Hilbert transforms of those of the primal DFB. Let us choose the $2\boldsymbol{\pi}$-periodic phase function $\phi_A(\boldsymbol{\omega})$ as follows:

$$\phi_A(\boldsymbol{\omega}) = \begin{cases} -\frac{\omega_1}{2} - \frac{\omega_2}{2} + \frac{\pi}{2}, & \omega_1 + \omega_2 > 0, \\ -\frac{\omega_1}{2} - \frac{\omega_2}{2} - \frac{\pi}{2}, & \omega_1 + \omega_2 < 0. \end{cases} \tag{11}$$

Fig. 2(a) illustrates the phase function $\phi_A(\boldsymbol{\omega})$ where black and white represent $-\pi/2$ and $\pi/2$, respectively.

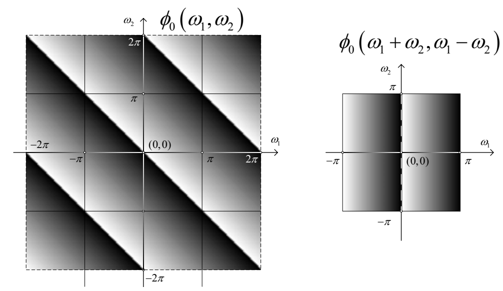

(a) $\phi_A(\boldsymbol{\omega})$ (b) $\phi_A(\boldsymbol{\omega}^{\boldsymbol{Q}})$

Fig. 2. The phase functions $\phi_A(\boldsymbol{\omega})$ and $\phi_A(\boldsymbol{\omega}^{\boldsymbol{Q}})$, black to white shades correspond to change of values from $-\pi/2$ to $\pi/2$.

It can be shown that the function $\phi_A(\boldsymbol{\omega}^{\boldsymbol{Q}})$ (see Fig. 2(b)) is a $(\pi, 2\pi)^T$-periodic function, and

$$\begin{aligned} \phi_A(\boldsymbol{\omega}^{\boldsymbol{Q}}) &= \phi_A(\omega_1 + \omega_2, \omega_1 - \omega_2), \\ &= \begin{cases} -\omega_1 + \frac{\pi}{2}, & 0 < \omega_1 < \pi, -\pi < \omega_2 < \pi, \\ -\omega_1 - \frac{\pi}{2}, & -\pi < \omega_1 < 0, -\pi < \omega_2 < \pi. \end{cases} \end{aligned}$$

Substituting $\phi_A(\boldsymbol{\omega}^{\boldsymbol{Q}})$ to equations (7) and (8) to evaluate $H^H_{dk}(\boldsymbol{\omega})$, $k = 0, 1$, we have yields

$$H^H_{dk}(\boldsymbol{\omega}) = \begin{cases} e^{-j\pi/2}H_{dk}(\boldsymbol{\omega}), & \omega_1 > 0, \\ e^{j\pi/2}H_{dk}(\boldsymbol{\omega}), & \omega_1 < 0. \end{cases} \tag{12}$$

Therefore, the dual filters $H^H_{dk}(\boldsymbol{z})$ are Hilbert transforms with respect to ω_1 of the primal filters $H_{dk}(\boldsymbol{z})$ for $k = 0, 1$.
Similarly, let $\phi_B(\boldsymbol{\omega})$ be defined as

$$\phi_B(\boldsymbol{\omega}) = \begin{cases} -\frac{\omega_1}{2} + \frac{\omega_2}{2} + \frac{\pi}{2}, & \omega_1 - \omega_2 > 0, \\ -\frac{\omega_1}{2} + \frac{\omega_2}{2} - \frac{\pi}{2}, & \omega_1 - \omega_2 < 0. \end{cases} \tag{13}$$

Following analogous derivation, the other two $H^H_{dk}(\boldsymbol{\omega})$ are

$$H^H_{dk}(\boldsymbol{\omega}) = \begin{cases} e^{-j\pi/2}H_{dk}(\boldsymbol{\omega}), & \omega_2 > 0, \\ e^{j\pi/2}H_{dk}(\boldsymbol{\omega}), & \omega_2 < 0. \end{cases} \tag{14}$$

Hence $H^H_{dk}(\boldsymbol{z})$ are Hilbert transforms with respect to ω_2 of $H_{dk}(\boldsymbol{z})$ for $k = 2$ and 3. We have shown that the four directional filters of the dual DFB $H^H_{dk}(\boldsymbol{z})$ are related to those in the primal DFB by Hilbert transform in ω_1 or ω_2. Let us consider one pair of filters $H_{d3}(\boldsymbol{z})$ and $H^H_{d3}(\boldsymbol{z})$. Assuming that $H_{d3}(\boldsymbol{z})$ has real coefficients and zero phase, it can be considered as a sum of two real functions symmetric through the origin as

$$H_{d3}(\boldsymbol{\omega}) = P(\boldsymbol{\omega}) + P(-\boldsymbol{\omega}), \tag{15}$$

where

$$P(\boldsymbol{\omega}) = \begin{cases} H_{d3}(\boldsymbol{\omega}), & 0 < \omega_2, \\ 0, & \omega_2 < 0. \end{cases} \tag{16}$$

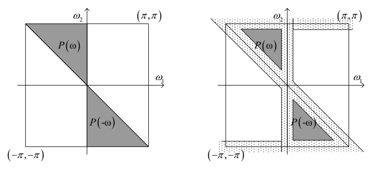

(a) (b) (c)

Fig. 3. (a) The ideal support regions of filter $H_{d3}(\boldsymbol{\omega})$, (b) The actual support of $H_{d3}(\boldsymbol{\omega})$ by realizable filters and, (c) $P(\boldsymbol{\omega})$ by definition in (16).

The ideal supports of $H^H_{d3}(\boldsymbol{z})$ and $P(\boldsymbol{z})$ are shown in Fig. 3(a), where black and white colors represent the passband and stopband. From (14), $H^H_{d3}(\boldsymbol{\omega})$ can be written as

$$H^H_{d3}(\boldsymbol{\omega}) = -jP(\boldsymbol{\omega}) + jP(-\boldsymbol{\omega}). \tag{17}$$

Hence $P(\boldsymbol{\omega}) = \frac{H_{d3}(\boldsymbol{\omega})+jH^H_{d3}(\boldsymbol{\omega})}{2}$.
In practice, the ideal support of the directional filter $H_{d3}(\boldsymbol{z})$ in Fig. 3(a) cannot be achieved, and the transition regions between the stopband and the passband (dotted areas in Fig. 3(b)) must be included. By the definition of $P(\boldsymbol{z})$ in (16), its support is illustrated in Fig. 3(c). We will show later that all but the aliasing components near $\omega_2 = \pm\pi$ of $P(\boldsymbol{z})$ can be cancelled in the two-level dual-tree fan FB.

For the synthesis side, the two synthesis fan filters of the prototype fan FB are used in both the primal and dual DFBs, except for the fan FBs at the second level of the dual DFB, which are modulated by $e^{j\phi_m(\boldsymbol{\omega})}$. Therefore, according to Theorem 1, both the primal and dual DFBs are PR. Assume that the synthesis filters have similar expressions as in (17). Let $F_{di}(\boldsymbol{z})$ and $F^H_{di}(\boldsymbol{z})$ be the synthesis filters of the primal and dual DFBs, respectively. We can write

$$G_{d3}(\boldsymbol{\omega}) = Q(\boldsymbol{\omega}) + Q(-\boldsymbol{\omega}), \tag{18}$$

$$G^H_{d3}(\boldsymbol{\omega}) = jQ(\boldsymbol{\omega}) - jQ(-\boldsymbol{\omega}). \tag{19}$$

$Q(\boldsymbol{z})$ is defined as the upper half of the directional filter $F_{d3}(\boldsymbol{z})$, i.e. $Q(\boldsymbol{\omega}) = F_{d3}(\boldsymbol{\omega})$ when $\omega_2 > 0$ and $Q(\boldsymbol{\omega}) = 0$ when $\omega_2 < 0$. Let us consider the two-channel FB created by $H_{d3}(\boldsymbol{z})$ and $H^H_{d3}(\boldsymbol{z})$ at the analysis side and $F_{d3}(\boldsymbol{z})$ and $F^H_{d3}(\boldsymbol{z})$ at the synthesis side with a decimation matrix $\boldsymbol{D}_2$ as shown in Fig. 4(a). Let $X(\boldsymbol{\omega})$ and $Y(\boldsymbol{\omega})$ denote the 2-D Fourier transforms of the input and the output reconstructed by this two-channel FB. Hence

$$Y(\boldsymbol{\omega}) = \frac{1}{2|\boldsymbol{D}_2|} \sum_{\mathbf{k}\in\mathcal{N}(\boldsymbol{D}_2^T)} X(\boldsymbol{\omega} - 2\pi\boldsymbol{D}_2^{-T}\mathbf{k}) \tag{20}$$
$$\Big(H_{d3}(\boldsymbol{\omega} - 2\pi\boldsymbol{D}_2^{-T}\boldsymbol{k})G_{d3}(\boldsymbol{\omega}) + H^H_{d3}(\boldsymbol{\omega} - 2\pi\boldsymbol{D}_2^{-T}\boldsymbol{k})G^H_{d3}(\boldsymbol{\omega})\Big),$$

where $\mathcal{N}(\boldsymbol{D}_2^T) = \{(0,0)^T, (0,1)^T, (1,0)^T, (1,1)^T\}$. Define the four transfer functions $T_{\boldsymbol{k}}(\boldsymbol{\omega})$ as follows:

$$T_{\boldsymbol{k}}(\boldsymbol{\omega}) = H_{d3}(\boldsymbol{\omega}-2\pi\boldsymbol{D}_2^{-T}\boldsymbol{k})G_{d3}(\boldsymbol{\omega})+H^H_{d3}(\boldsymbol{\omega}-2\pi\boldsymbol{D}_2^{-T}\boldsymbol{k})G^H_{d3}(\boldsymbol{\omega}).$$

Except for when $\boldsymbol{k} = (0,0)^T$, $T_{\boldsymbol{k}}$ are called aliasing transfer functions. The structure is shift-invariant if the aliasing transfer functions are zero. Since $\boldsymbol{D}_2^{-T} = 0.5\boldsymbol{I}$, the aliasing transfer function associated with $\boldsymbol{k}$ is

$$\begin{aligned} T_{\boldsymbol{k}}(\boldsymbol{\omega}) &= H_{d3}(\boldsymbol{\omega} - \pi\boldsymbol{k})G_{d3}(\boldsymbol{\omega}) + H^H_{d3}(\boldsymbol{\omega} - \pi\boldsymbol{k})G^H_{d3}(\boldsymbol{\omega}), \\ &= (P(\boldsymbol{\omega} - \pi\boldsymbol{k}) + P(-\boldsymbol{\omega} - \pi\boldsymbol{k}))\,(Q(\boldsymbol{\omega}) + Q(-\boldsymbol{\omega})) + \\ &\quad + (-jP(\boldsymbol{\omega} - \pi\boldsymbol{k}) + jP(-\boldsymbol{\omega} - \pi\boldsymbol{k}))\,(jQ(\boldsymbol{\omega}) - jQ(-\boldsymbol{\omega})), \\ &= 2P(\boldsymbol{\omega} - \pi\boldsymbol{k})Q(\boldsymbol{\omega}) + 2P(-\boldsymbol{\omega} - \pi\boldsymbol{k})Q(-\boldsymbol{\omega}). \end{aligned} \tag{21}$$

Note that $Q(\boldsymbol{z})$ has the same passband and stopband as those of

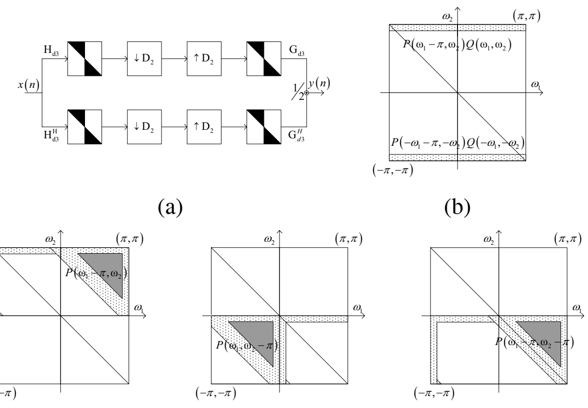

(a) (b)

(c) (d) (e)

Fig. 4. (a) Subband 3 of the two-channel dual-tree fan FB considered separately from the tree. (b) The frequency supports of the significant aliasing transfer function in (21), which corresponds to $\boldsymbol{k} = (1,0)^T$. The frequency support of $P(\boldsymbol{\omega}-\pi\boldsymbol{k})$: (c) $\boldsymbol{k} = (1,0)^T$, (d) $\boldsymbol{k} = (0,1)^T$, and (e) $\boldsymbol{k} = (1,1)^T$.

$P(\boldsymbol{z})$ depicted in Fig. 3(c). It is evident that the aliasing is significant only if $Q(\boldsymbol{\omega})$ and $P(\boldsymbol{\omega} - \pi\boldsymbol{k})$ have overlapping transition or passband regions. Therefore, it can be concluded from the supports of $P(\boldsymbol{\omega}-\pi\boldsymbol{k})$ in Figs. 4(c), (d) and (e) that $T_{\boldsymbol{k}}(\boldsymbol{\omega})$ with $\boldsymbol{k} = (1,0)^T$ is the only significant aliasing transfer function. The frequency supports of this transfer function are the dotted regions in Fig. 4(b). In order to have a translation invariant image transform, a pyramidal decomposition is used to remove the frequency components in these regions before applying the signal to the dual-tree DFB.

3. THE COMPLEX DIRECTIONAL PYRAMID

In order to construct a shift-invariant multiscale and multidirectional decomposition, a combination of a multiresolution FB with the dual-tree DFB at every highpass resolution is proposed. The multiscale FB consists of an undecimated two-channel FB and an iterated Laplacian pyramid. Consider the construction in Fig. 5. At the front end, an undecimated two-channel FB ($L_0(\boldsymbol{\omega})$ and $R(\boldsymbol{\omega})$) is used to separate the high frequency components near $(\pi,.)$ and $(.,\pi)$, which potentially cause aliasing in the dual-tree (see Fig. 4(b)). The highpass filter $R(\boldsymbol{\omega})$ produces a 'residual' image similar to that in the steerable pyramid [2]. It is clear that, for this undecimated FB to be PR, the filters must satisfy

$$|R(\boldsymbol{\omega})|^2 + |L_0(\boldsymbol{\omega})|^2 = 1. \tag{22}$$

The output of the wide-band lowpass filter $L_0(\boldsymbol{\omega})$ is then fed into the first stage of the Laplacian pyramid where the signal is divided into two parts: the coarse approximation (point L in Fig. 5(a)) and high frequency component (point H in Fig. 5(a)). This high frequency component is then further decomposed by a dual-tree of DFB to produce the real and imaginary value of 2^n complex directional subbands.
The aliasing effect of the pyramidal DFB is analyzed in [7] by viewing it as an overcomplete FB. The aliasing effect of the conventional DFB and the Laplacian pyramid to the equivalent directional filters is considered, and the condition to reduce this effect is that the two

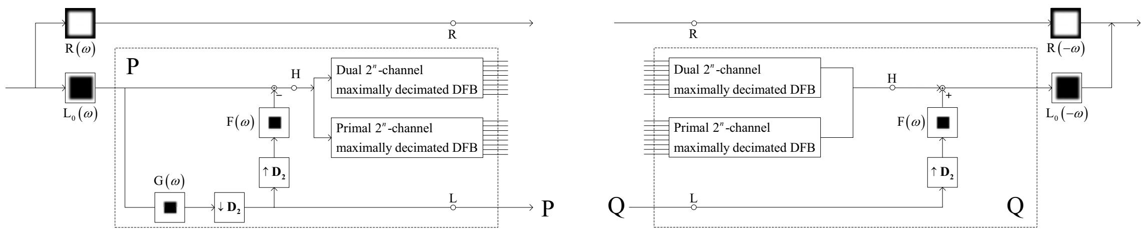

(a) (b)

Fig. 5. A shift-invariant pyramid: (a) Analysis side, and (b) Synthesis side. Similar P and Q blocks can be reiterated at lower scale to decompose an image into a multiscale representation.

Laplacian filters ($G_1(\boldsymbol{\omega})$ and $G_2(\boldsymbol{\omega})$ in Fig. 5) should satisfy the Nyquist criterion. This condition means that the frequency responses of the two filters should have the passband regions (including the transition bands) strictly limited in $[-\pi/2, \pi/2]^2$. The $G_1(\boldsymbol{\omega})$ and $G_2(\boldsymbol{\omega})$ in this paper satisfy this designed constraint. Consequently, there is no aliasing in the coarse approximation (L) and its spectrum near π is negligible, and therefore minimizes the potential aliasing from the dual-tree DFB in the second level of the pyramid. Since the Laplacian pyramid used in the structure is shown to provide subband images with no aliasing, it is called a *shift-invariant* Laplacian pyramid.

The dual-tree PDFB of the directional complex pyramid is a shift-invariant Laplacian pyramid cascaded with a dual-tree of 2^n-channel DFBs at each high resolution level of the pyramid. The first resolution is illustrated in Fig. 5. The block P and Q are iterated to provide a multiscale decomposition and synthesis.

The dual-tree of 2^n-channel DFBs is constructed by cascading two similar two-channel FBs into every corresponding branches of the two DFBs in the dual-tree 2^{n-1}-channel DFBs. The frequency supports of these two-channel FBs and implementation method are similar to those of the conventional DFB in [5]. By this construction, the resulting directional filters in the primal and dual DFBs satisfy the same condition in (12) or (14). Therefore, the equivalent directional filters at all directions in the dual DFB are always the Hilbert transforms of the corresponding filters in the primal DFB in ω_1 or ω_2. It is shown in the previous section that some of the aliasing components in the dual-tree four-band DFB are cancelled out. That discussion on aliasing cancellation between the dual and primal subbands can be directly extended to the directional subbands of the dual-tree DFB with 2^n subbands. Furthermore, the frequency components at the aliasing region in Figure 4(b) are already removed by the multiscale Laplacian pyramid before the dual-tree DFB. Therefore, the overall FB is shift-invariant.

An implementation of the dual-tree PDFB and its shift-invariance performance can be found in [6]. The frequency responses of one corresponding directional filter in the primal DFB, dual DFB, and complex DFB are illustrated in Fig 6. If the impulse responses of the primal and dual directional filters are denoted as $h_P(\boldsymbol{n})$ and $h_D(\boldsymbol{n})$, then the complex filter is determined by $h_C(\boldsymbol{n}) = 0.5(h_P(\boldsymbol{n}) + jh_D(\boldsymbol{n}))$.

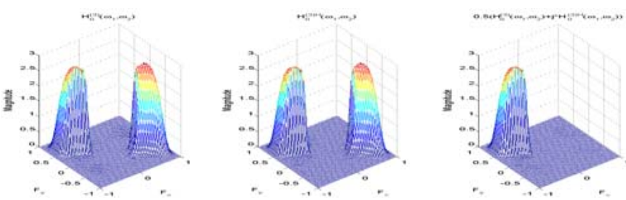

(a) (b) (c)

Fig. 6. The frequency response of equivalent directional filters of a dual-tree PDFB implementation in [6]. (a) A directional filter of the primal PDFB,(b) The corresponding filter of the dual PDFB, and (c) The complex filter.

4. CONCLUSION

A novel shift-invariant multiscale multidirectional image transform implemented by the dual-tree PDFB is presented in this work. The image decomposition offered by the FB has many of the desire properties for image analysis. It is multiscale, multidirectional and nearly shift-invariant, and has very low overcomplete ratio. The number of directional subbands in the proposed FB can be increased adaptively depending on image features without increasing the redundancy of the representation. Furthermore, the decomposition provides phase information on the image feature, which can be very useful in several image processing tasks, such as motion estimation or edge detection. Last but not least, the whole framework can be efficiently implemented by separable filters as described in [6].

5. REFERENCES

[1] G. Strang and T. Q. Nguyen, *Wavelets and Filter Banks*. Wellesley Cambridge, 1996.

[2] E. P. Simoncelli, W. T. Freeman, E. H. Adelson, and D. J. Heeger, “Shiftable multiscale transform,” *IEEE Transaction on Information Theory*, vol. 38, no. 2, pp. 587–607, Mar 1992.

[3] P. Vaidyanathan, *Multirate Systems and Filter Banks*. Prentice-Hall,Englewood Cliffs, NJ, 1993.

[4] N. G. Kingsbury, “Image processing with complex wavelets,” *Phil. Trans. Royal Society London A*, vol. 357, no. 1760, pp. 2543–2560, Sept 1999.

[5] R. H. Bamberger and M. J. T. Smith, “A filter bank for the directional decomposition of images: theory and design,” *IEEE Transactions on Signal Processing*, vol. 40, no. 7, pp. 882 –893, Apr. 1992.

[6] T. T. Nguyen and S. Oraintara, “The shift-invariant complex directional pyramid,” *Submitted to the IEEE Transaction on Image Processing*, Oct 2005.

[7] ——, “On the aliasing effect of the contourlet filter banks,” in *Submitted to the International Symposium on Circuits and Systems (ISCAS’06)*, Oct. 2005.